

$A_2Cu_2CoO_2S_2$ (A = Sr, Ba), A Novel Example of a Square-Planar CoO_2 Layer

W. J. Zhu* and P. H. Hor*

Department of Physics and Texas
Center for Superconductivity
University of Houston, Houston, Texas 77204-5932

A. J. Jacobson,* G. Crisci, T. A. Albright, and S.-H. Wang

Department of Chemistry and Texas
Center for Superconductivity
University of Houston, Houston, Texas 77204-5641

T. Vogt

Physics Department, Brookhaven National Laboratory
Upton, New York 11973

Received July 28, 1997

Layered transition-metal oxides and sulfides with square metal anion lattices have been extensively studied because of their unusual electronic and magnetic properties. Novel insulator metal transitions, superconductivity, and charge-density waves have been observed in these layered materials.¹ Only a few studies have examined layered late-transition-metal oxychalcogenides that are composed of transition-metal oxide and transition-metal chalcogenide layers. The first reported example, $Na_{1.9}Cu_2Se_2Cu_2O$,^{2,3} exhibits metallic behavior below 250 K. Combinations of transition-metal oxide and chalcogenide layers are of interest because of possible novel electronic and magnetic properties resulting from interactions between the two types of layers. Here, we report the synthesis and characterization of the first layered cobalt oxysulfides, $A_2Cu_2CoO_2S_2$ (A = Sr, Ba), which contain unusual square-planar CoO_2 layers. The compounds show successive magnetic transitions and spin-glass behavior at low temperatures.

The compounds $A_2Cu_2CoO_2S_2$ (A = Sr, Ba) were synthesized by reaction of SrS/BaS, Co, and CuO.⁴ The structure of Sr_2-

(1) (a) Sleight, A. W. *Science* **1988**, *242*, 1519–1727. (b) Martinson, L. S.; Schweitzer, J. W.; Baenziger, N. C. *Phys. Rev. Lett.* **1993**, *71*, 125–128. (c) Fleming, R. M.; Ter Haar, L. W.; DiSalvo, F. J. *Phys. Rev. B* **1987**, *35*, 5388–5391.

(2) Park, Y.; Degroot, D. C.; Schindler, J. L.; Kannewurf, C. R.; Kanatzidis, M. G. *Chem. Mater.* **1993**, *5*, 8–10.

(3) For theory on this compound, see: Chacon, G.; Long, X.; Cheng, C. *J. Alloys Compds.* **1994**, *216*, 177–182.

(4) (a) Sample preparation: for $Sr_2Cu_2CoO_2S_2$, a quartz tube containing pellets with SrS (2.00 mmol), Co (1.00 mmol), and CuO (2.00 mmol) was evacuated and sealed. The tube was heated at 825 °C for 24 h. The sample was then reground, pelletized, and heated for additional 24 h followed by furnace cooling. A black single-phase sample was obtained. For $Ba_2Cu_2CoO_2S_2$, the reaction temperature was 850 °C. Its color was dark brown. Both compounds are stable in air. Single-crystal $Sr_2Cu_2CoO_2S_2$ was grown with stoichiometric amounts of SrS, Co, and CuO (~2 g total). The mixture sealed in a quartz tube was heated at 200 °C/h to 1150 °C, held for 2 h, cooled to 950 °C at 5 °C/h and then furnace cooled to ambient temperature. Several black plate-like crystals that grew in the cavities were separated from the matrix. (b) Crystal data and structure determination: $Sr_2Cu_2CoO_2S_2$, single-crystal X-ray, fw 457.37, space group $I4mmm$, $a = 3.981(1)$ Å, $c = 17.625(4)$ Å, $V(\text{Å}^3) = 279.33(12)$, $Z = 2$, $R_1 = 3.7\%$, $wR_2 = 8.8$, $GOF(F^2) = 1.2$. Powder neutron diffraction: data collected at 25 °C on the high-resolution diffractometer at the National Institute of Standards and Technology over the range $10^\circ < 2\theta < 165^\circ$, stepsize 0.05° , $\lambda = 1.5402$ Å. The data were analyzed by the Rietveld method using the GSAS programs:^{4c} $a = 3.9880(1)$ Å, $c = 17.6790(5)$ Å, $V(\text{Å}^3) = 281.17(2)$, $wR_p = 6.32\%$, $R_p = 5.10\%$, $\chi^2 = 1.74$. X-ray powder diffraction data for $Ba_2Cu_2CoO_2S_2$ were collected at 25 °C with Cu K_α radiation, $15^\circ < 2\theta < 105^\circ$ at stepsize 0.03° and were analyzed by Rietveld refinement using the program DBW.^{4d} $a = 4.0562(8)$ Å, $c = 18.844(4)$ Å, $V(\text{Å}^3) = 310.04(19)$, $wR_p = 6.50\%$, $R_p = 4.82\%$, $GOF = 0.91$. (c) Larson, A. C.; Von Dreele, R. B. General Structure Analysis System, LANSCE, MS-H805, Los Alamos National Laboratory, Los Alamos, NM 87545. (d) Young, R. A.; Sakthivel, A.; Moss, T. S.; Paiva-Santos, C. O. *J. Appl. Crystallogr.* **1995**, *28*, 366–367.

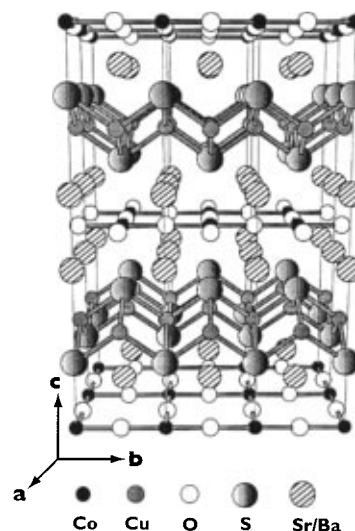


Figure 1. Structure of $A_2Cu_2CoO_2S_2$ (A = Sr, Ba), showing alternate stacking of the CoO_2 and Cu_2S_2 layers. Selected atomic distances (Å) for $Sr_2Cu_2CoO_2S_2$ from single-crystal X-ray data: Co–O, 1.9905(5); Co–S, 3.008(1); Cu–S, 2.432(2); Sr–O, 2.5776(7); Sr–S, 3.1311(13).

$Cu_2CoO_2S_2$ was determined by single-crystal X-ray diffraction and found to be isostructural with $Sr_2Mn_3As_2O_2$ ⁵ (see Figure 1). The distribution of Cu and Co ions between the two layers in $Sr_2Cu_2CoO_2S_2$ was determined by powder neutron diffraction. Surprisingly, the cobalt cations were found only in the square-planar oxide layer, while Cu is located in the anti-PbO type Cu_2S_2 layer. The refinements of the single-crystal X-ray and the neutron diffraction data both indicate an anomalously large thermal parameter, U_{Cu} , for the Cu atom. A similar result was obtained from the refinement of the X-ray powder data for $Ba_2Cu_2CoO_2S_2$. Further refinements of the Cu site occupancy using both sets of $Sr_2Cu_2CoO_2S_2$ diffraction data suggested that the large U_{Cu} might be due to a small Cu deficiency. Refinements in which U_{Cu} was fixed at a value equal to U_{Co} gave comparable Cu deficiencies of ~5%. Refinements of various other structure models including site mixing of Cu and Co atoms and displacement of the Cu atom from its ideal position were not successful in reducing U_{Cu} . To confirm the possibility of Cu nonstoichiometry, a pure phase with a 12.5% Cu deficiency, $Sr_2Cu_{1.75}CoO_2S_2$, was synthesized.⁴ The lattice parameters of this compound, determined by X-ray diffraction with silicon as an internal standard, contract by 0.15% for the a axis and by 0.23% for the c axis relative to the parent “stoichiometric” phase. While a small Cu deficiency in $Sr_2Cu_2CoO_2S_2$ seems the most likely explanation for the present data, other more subtle structural effects are possible and will be investigated further by electron diffraction.

The $A_2Cu_2CoO_2S_2$ (A = Ba, Sr) phases are, to our knowledge, the first examples of a square-planar CoO_2 layer. The square-planar MO_2 layer has previously been reported for M = Cu, Ni, Mn, and Zn in the compounds Nd_2CuO_4 ,⁶ $LaNiO_2$,⁷ $Sr_2Mn_3As_2O_2$,⁵ and $Ba_2Zn_3As_2O_2$,⁸ respectively. Tight binding calculations with an extended Hückel Hamiltonian⁹ were carried out to examine the electronic structure of the new phases. Since

(5) (a) Brechtel, E.; Cordier, G.; Schäfer, H. *Z. Naturforsch. B* **1979**, *34*, 777–780. (b) Stetson, N. T.; Kauzlarich, S. M. *Inorg. Chem.* **1991**, *30*, 3969–3971.

(6) Müller-Buschbaum, H.; Wallschläger, W. *Z. Anorg. Allg. Chem.* **1975**, *414*, 76–80.

(7) Crespín, M.; Levitz, P.; Gatineau, L. *J. Chem. Soc., Faraday Trans.* **1983**, *79*, 1181–1194.

(8) Brock, S. L.; Kauzlarich, S. M. *Inorg. Chem.* **1994**, *33*, 2491–2492.

(9) The calculations for the density of state used a 300 K point set with the standard atomic parameters taken from S. Alvarez (private communication). Full details of the computations will be forthcoming.

Cu is more electronegative than Co, one would expect that the Cu 3d based levels will lie at lower energy than those derived from Co 3d. However, the O and S atomic orbitals destabilize and split the Cu and Co 3d levels as given by their local coordination geometries. The Cu levels are consequently split into a three above two (t_2 and e) pattern consistent with the tetrahedral environment. Antibonding from the S lone pairs serves to push the t_2 set to moderately high energies, and it is these crystal orbitals that contribute at the Fermi level. The Co 3d orbitals are antibonding to the O lone pairs and split into a pattern consistent with the square-planar geometry. At the highest energy is an empty band of Co $3d_{x^2-y^2}$ (where the x , y , and z axes correspond to the a , b , and c axes, respectively, in Figure 1) antibonding to the O lone pairs in a σ sense. The remaining Co 3d levels lie in the vicinity of the Cu t_2 set. The basic electronic structure then is a slightly larger than d^7 square-planar Co layer and a slightly less than d^{10} tetrahedral Cu layer. The exact details are very sensitive to the lattice dimensions and parameters used in the calculation. In the structure of $\text{Sr}_2\text{Cu}_2\text{CoO}_2\text{S}_2$, the Co–S (apical) distance (3.008(1) Å) is much longer than a typical bond (2.36 Å in BaCoS_2^{10}), indicating only very weak Co–S bonding between CoO_2^{2-} and $\text{Cu}_2\text{S}_2^{2-}$ layers. This is also consistent with our calculations. The Cu–S distance (2.432(1) Å) in the structure unit Cu_2S_2 is comparable to the value of its many related copper sulfides (e.g., 2.413 Å in $\text{BaCu}_2\text{S}_2^{11}$).

The electrical conductivity of the polycrystalline sample $\text{Sr}_2\text{Cu}_2\text{CoO}_2\text{S}_2$ measured by the standard four-probe method shows semiconducting behavior with a resistivity of about 4 Ω cm at 300 K. This is about 10 thousand times lower than that of the pure Ba-containing analogue $\text{Ba}_2\text{Cu}_2\text{CoO}_2\text{S}_2$. The more Cu-deficient sample $\text{Sr}_2\text{Cu}_{1.75}\text{CoO}_2\text{S}_2$ has a lower resistivity than that of $\text{Sr}_2\text{Cu}_2\text{CoO}_2\text{S}_2$. The resistivity also can be modified by aliovalent doping. Partial substitution of La^{3+} for Sr^{2+} and Na^+ for Sr^{2+} increases and decreases, respectively, the electrical conductivity. The magnetic susceptibility data (see Figure 2) show successive broad maxima for both compounds, suggesting low dimensional antiferromagnetic transitions of the Co^{2+} cations. The Ba-containing phase shows broad peaks at 160 and 225 K with no difference between field cooling (fc) and zero-field (zfc) cooling. The Sr-containing phase, on the other hand, shows a more complicated behavior. In addition to two broad transitions at about 100 and 200 K, a crossover, possibly antiferromagnetic to ferrimagnetic transition, takes place at about 80 K as indicated in the fc data. The difference observed

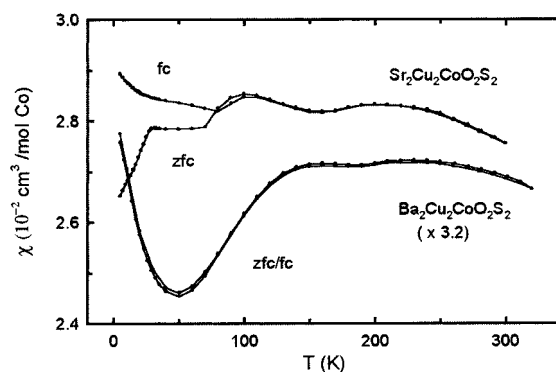


Figure 2. Zero-field and field-cooled magnetic susceptibilities for $\text{A}_2\text{Cu}_2\text{CoO}_2\text{S}_2$ ($\text{A} = \text{Sr}, \text{Ba}$) measured at 0.5 T. The data for $\text{A} = \text{Ba}$ were multiplied by a factor of 3.2.

between fc and zfc susceptibilities beginning at this temperature suggests spin-glass freezing of ferrimagnetic clusters. At temperatures below 30 K, the fc susceptibility is enhanced, while that of zfc again exhibits a freezing behavior. The magnetic behaviors of $\text{A}_2\text{Cu}_2\text{CoO}_2\text{S}_2$ ($\text{A} = \text{Sr}, \text{Ba}$) above 80 K are similar to that of $\text{La}_2\text{CoO}_4^{12}$ which also shows successive antiferromagnetic transitions.

Additional single-crystal neutron scattering studies are necessary to solve the detailed magnetic structure and its temperature dependence. The synthesis of these layered transition-metal oxychalcogenides, $\text{A}_2\text{Cu}_2\text{CoO}_2\text{S}_2$ ($\text{A} = \text{Sr}, \text{Ba}$), suggests a new approach to other novel phases with perovskite oxide layers stacked with the fluorite type copper chalcogenide layers $\text{Cu}_{2n}\text{Q}_{n+1}$ ($\text{Q} = \text{S}, \text{Se}$). Preliminary results with other elements do indicate the formation of such a broad class of new materials. Further studies are underway to explore new electronic and magnetic properties in this system.

Acknowledgment. This work was supported by NSF (DMR 9122043, DMR-9214804), ARPA Grant MDA 972-90-J-1001, the Texas Center for Superconductivity at the University of Houston, the Robert A. Welch Foundation, and the Advanced Research Program as administered by the Texas Higher Education Coordination Board.

Supporting Information Available: Tables of atomic coordinates, isotropic displacement parameters, selected bond lengths and angles for $\text{A}_2\text{Cu}_2\text{CoO}_2\text{S}_2$ ($\text{A} = \text{Sr}, \text{Ba}$) based on the X-ray and neutron diffraction data, and the observed and calculated powder diffraction patterns for $\text{A}_2\text{Cu}_2\text{CoO}_2\text{S}_2$ (6 pages). See any current masthead page for ordering and Internet access instructions.

JA972542V

(10) Snyder, G. J.; Gelabert, M. C.; DiSalvo, F. J. *J. Solid State Chem.* **1993**, *113*, 355–361.

(11) Ouammou, A.; Mouallem-Bahout, M.; Pena, O.; Halet, J.-F.; Saillard, J.-Y.; Carel, C. *J. Solid State Chem.* **1995**, *117*, 73–79.

(12) Yamada, K.; Matsuda, M.; Endoh, Y.; Keimer, B.; Birgeneau, R. J.; Onodera, S.; Mizusaki, J.; Matsuura, T.; Shirane, G. *Phys. Rev. B* **1989**, *39*, 2336–2342.